HardwareX 16 (2023) e00474

Contents lists available at ScienceDirect

HardwareX

journal homepage: www.elsevier.com/locate/ohx

Low-speed instrumented drill press for bone screw insertion

J. Logan Betts [a,b], Frank M. Brinkley [a,b], Lauren B. Priddy [c], Matthew W. Priddy [a,b,*]

[a] Department of Mechanical Engineering, Mississippi State University, Mississippi State, MS 39762, United States of America
[b] Center for Advanced Vehicular Systems, Mississippi State University, Starkville, MS 39759, United States of America
[c] Department of Agricultural and Biological Engineering, Mississippi State University, Mississippi State, MS 39762, United States of America

ARTICLE INFO

Keywords:
Screw insertion
Open source hardware
Arduino
Orthopedic fixation devices
Osteointegration
Mechanical testing

ABSTRACT

Screw insertion torque is a widely used/effective method for quantifying fixation strength in orthopedic implant research for different screw geometries, implantation sites, and loads. This work reports the construction of an open-source instrumented benchtop screw insertion device for a total cost of $7545 ($492 + $7053 for equipped sensors), as well as validation of the device and an example use-application. The insertion device is capable of recording the axial load, rotational speed, and applied torque throughout the screw insertion process at 10 samples per second, as demonstrated in the validation test. For this combination of bone analog (20 PCF Sawbones©), screw, and loading, the resolution of the torque sensor was 25% of the maximum measured torque; a different model torque sensor would be required to meet ASTM F543-17, which specifies a resolution of 10% of the maximum torque. This system is optimized for fastener insertion at speeds of 120 rpm or less and axial loading up to 50 N.

Specifications table

Hardware name	Instrumented Low-Speed Drill Press
Subject area	Educational tools and open source alternatives to existing infrastructure
Hardware type	Measuring physical properties and in-lab sensors
Open source license	CERN Open Hardware Licence Version 2 - Permissive
Cost of hardware	$7545 ($492 + $7053 for equipped sensors)
Source file repository	https://doi.org/10.17605/OSF.IO/X3EKH

1. Hardware in context

Bone screw success for long-term fixation is correlated to insertion characteristics including insertion torque. Bone screws are used extensively in orthopedic surgeries to stabilize bone fractures and provide rigid fixation when used with plates [1]. The AO Cortex screw utilizes a buttress thread geometry and has been the standard for fixation since the late 1950's [2]. However, recent research on bone fasteners has shifted to tailoring geometric parameters such as thread count, pitch, and diameter for specific applications such as different types of bone and implantation sites for fracture stabilization [3,4], as well as dental and spinal implants [5–7]. The study of bone screws requires an understanding of insertion mechanics, especially for screws incorporating self-tapping cutting flutes; the effectiveness of a particular screw design is dependent on the interface between the bone screw and peri-implant bone.

* Corresponding author at: Department of Mechanical Engineering, Mississippi State University, Mississippi State, MS 39762, United States of America.
. Matthew W. Priddy (M.W. Priddy).
E-mail address: mwpriddy@me.msstate.edu (M.W. Priddy).

https://doi.org/10.1016/j.ohx.2023.e00474
Received 12 May 2022; Received in revised form 24 May 2023; Accepted 7 September 2023
Available online 18 September 2023

Table 1
Hardware summary.

Speed range	Max torque	Max down-force	Vertical clearance
20–80 rpm	18 N-m	200 N	approx. 150 mm

Historically, this understanding has been derived from experiments using bone analogs such as polyurethane foam, and comparing pullout strength between different implant designs [8,9]. This has led to an understanding of the global response, but experiments have provided few methods to measure the stress–strain response at the interface of the implant and peri-implant bone. Finite element analysis has demonstrated the ability to create high fidelity simulations of the screw insertion process and provide insight into mechanical loading at this interface [10,11]. However, experimental data (e.g., torque, rotation, axial load vs. time) is required to accurately create such simulations and calibrate material models [12]. Therefore, an experimental apparatus is needed to measure insertion characteristics such as torque vs. time, and axial force, to effectively compare different bone screws.

Maximum insertion torque (MIT) and pullout strength (POS) have long been widely accepted methods to evaluate bone screw fixation strength [9,13,14]. Despite many attempts to determine the most appropriate metric for assessment, it has become commonplace to report both metrics since the significance of each can vary depending on the application and condition of bone. The advantage of reporting both metrics is highlighted in previous research, showing that over torquing leads to a compromised POS [15–17]. While many researchers have access to commercial testing equipment for insertion and pullout testing (e.g., tension test frames, with axial add-ons), devices capable of combined axial and large-angle torque (e.g., multiple rotations) loading are cost prohibitive ($100,000+). This has led many researchers to build custom apparatuses to measure torque during the screw insertion process, but often, information on the design, construction, and/or operation is lacking. There is a need for a low-cost open-source testing apparatus to provide a method for collecting torque versus time data, for both experimental characterization and calibration of finite element simulations.

The objective of this paper was to aid other researchers by clearly presenting the design and construction details of an apparatus to measure insertion torque and axial force during the screw insertion process. The selection of the sensor and other components were based on our specific application and sensors already on hand; however the design is intended to be customizable to specific experimental requirements and could utilize a different rotary torque sensor or load cell to further reduce the cost. The goal of this work was to reduce the overall cost of the screw insertion system as compared to those that are commercially available.

2. Hardware description

This system is a modified drill press that has been customized to facilitate instrumented, low-speed screw insertion. The insertion torque, down-force, rotation speed, and number of rotations are recorded and plotted during testing. While this apparatus has been specifically designed to meet the requirements for insertion of bone screw fasteners, other instrumented screw insertion and setups can be implemented by reprogramming the motor speeds and increasing the setup height by replacing the drill press column. The quick-change bit holder on the torque sensor will accommodate any standard 1/4” hex shaft bit. Table 1 provides a summary of the hardware capabilities.

2.1. Drill press

This apparatus utilizes a compact drill press stand designed for holding handheld power drills. A typical drill presses uses an AC motor in a belt drive setup optimized for wood cutting (3000 rpm) or metal cutting (300 rpm). To achieve the necessary low speeds of 20–80 rpm for the intended application, this setup uses a geared stepper motor from StepperOnline with a 15:1 gear ratio with an accompanying stepper motor driver from the same manufacturer. The motor mounts to the drill press stand using a motor standoff and custom faceplate. The motor speed and direction are controlled with a three button control board and power switch. The speed button allows selection of four (4) discrete speeds (OFF, LOW, MED, and HI) which are programmed as 0, 20, 40, 80 revolutions per minute (rpm) for this study, respectively. The switch status is monitored by the Arduino to loop through the four (4) speeds and rotation direction (clockwise or counterclockwise) by using the built-in pull-up resistors for the respective digital pins in the Arduino. The control board also has five (5) LEDs — three (3) red LEDs for motor speed and two (2) yellow LEDs for direction — to indicate the current motor settings. An on–off rocker switch is used to toggle the motor on or off. Motor speed, direction, and on/off status are digitally controlled by the Arduino. A 24-volt power supply powers the motor, and an Arduino Mega 2560 microcontroller commands the stepper motor driver. A buck converter is used to step down the 24-volt supply to 5 V to supply power to the Arduino. All electronics components are housed in a 400 by 300 by 120 mm Acrylonitrile butadiene styrene (ABS) housing on two (2) rows of DIN 3 rail.

Similar to other drill presses, the upper portion of the drill press is able to slide up and down the length of the main shaft to allow for a variety of drill attachment and work piece sizes. The drill portion has a spring loaded return with a travel of approximately six (6) inches. The press comes standard with a six (6) inch handle to apply down pressure, but this setup has replaced the handle with a 12 inch diameter wheel with a counterweight system to apply repeatable down-pressure. Users can also use the wheel without the counterweights similarly to the default handle with the same mechanical advantage. The drill press base is slotted to accept fixturing such as a vice and permit adjustment of the workpiece for proper alignment. A keyless drill chuck and driveshaft are connected to the stepper motor with the driveshaft supported above and below the load cell using oil-impregnated brass bushings. The length of the shaft allows for the chuck to contact the lower bushing and transfer the compressive force into the force sensor.

Table 2
Design file overview.

Design filename	File type	Open source license	Location of the File
AdapterCap-3Dprint	CAD File	CERN-OHL-P V2	https://osf.io/28yst/
SensorAdapter-3DPrint	CAD File	CERN-OHL-P V2	https://osf.io/fgy47/
ScrewInsertion-REVB	CAD File	CERN-OHL-P V2	https://osf.io/ac2js/
12 mm shaft	CAD File	CERN-OHL-P V2	https://osf.io/qv32b/
Clamping plate	CAD File	CERN-OHL-P V2	https://osf.io/w35rt/
Nema23 faceplate	CAD File	CERN-OHL-P V2	https://osf.io/ks9ct/
StepperControl	Arduino File	CERN-OHL-P V2	https://osf.io/a2c6j/
Assembly animation	Video		https://osf.io/qtsua/

2.2. Force and torque sensors

The down-force applied during drilling is measured with a FUTEK© LTH300 through-hole load cell. The load cell is secured to the drill press frame, in-line with the motor shaft, with a 3D-printed housing. The torque, speed, and total number of rotations are measured with a FUTEK© TRH605 non-contact hex-drive rotary torque sensor with encoder. The torque sensor is mounted in the keyless chuck with the necessary bit held in the 1/4" hex drive quick-coupler. The TRH605 is rated for 18 N-m and 7000 rpm. The torque sensor and load cell are each connected to a FUTEK© USB520 signal conditioner that have been calibrated by FUTEK© for each sensor. The signal conditioners are connected to the recording PC via USB. Both sensors come with a copy of FUTEK's SENSIT© software and provides documentation for users who wish to integrate these sensors with different software such as LabVIEW or Python. The USB250 is capable of sampling rates of 5-4800 samples/sec for both sensors. The load cell has an combined error of 0.87% of rated output. The TRH605 torque sensor has a combined error of 0.30% of rated output. The breakdown of the specified errors can be found on the data sheet for each sensor.

Other researchers have used a variety of custom devices to measure the insertion torque and compressive force applied during the insertion of medical screws into *ex vivo* bone and common bone analogs such as SAWBONES® [8,18–21]. Little information is provided regarding operation procedures for these devices or how to reproduce them. Some systems measure only axial load [18]. Other systems use a wired torque sensor that limits the total number of rotations [8] or measures only the maximum insertion torque [9]. The system presented in this work utilizes a contactless torque sensor with a rotary encoder capable of measuring torques up to 18 N-m, rotational speeds up to 7000 rpm, and total rotational angle (unlimited). Additionally, mounting the axial force and torque sensor in the drill press frame minimizes fixturing limitations such as a permanent vise or work-holding position.

While this setup is primarily being used for bone screw characterization, this hardware can be used and modified to perform other tasks, including:

- measurement and comparison of screw insertion characteristics as a function of thread count, pitch, and diameter
- comparison of screw geometry insertion characteristics
- low speed screw insertion
- calibration and validation of finite element simulations of screw insertion

3. Design files

3.1. Design files summary

The design files are available in the project repository and summarized in Table 2. The adapter and cap are 3D printed components used to hold the force sensor and center the driveshaft. The assembly CAD file provides an overview of all modified components on the drill press stand. The video provides an animated order of assembly operations from the isometric exploded view. The 12 mm shaft is a threaded steel rod that connects the stepper motor to the Jacob's chuck. The clamping plate and NEMA23 faceplate are CAD files showing the dimensions and hole locations for the two adapter plates. StepperControl is a Arduino program that should be loaded onto the Arduino which controls the stepper motor.

4. Bill of materials

This section presents the off-the-shelf components and materials required to build the low-speed insertion device. Tables 3 and 4 summarizes the required parts and cost of the apparatus. To stay concise, the recommended locations for purchase and additional details are listed only in the file on the repository. The extended Bill of Materials can be found in the project repository here.

5. Build instructions

Caution: Throughout the build process protect yourself with appropriate PPE and review safety procedures & instructions before using any tools, or listed components.

Table 3
Mechanical bill of materials summary.

Component	Qty	Cost per unit (USD)	Total cost (USD)
Drill press stand	1	46.99	46.99
Arduino DIN rail mount	1	35.00	35.00
Driveshaft coupler	1	8.99	8.99
Stepper motor mount	1	19.99	19.99
3-Inch vise	1	14.36	14.36
Electronics enclosure	1	48.99	48.99
Driveshaft sleeve bushings	2	2.35	4.70
M4 × 0.7 by 85 mm screw	pkg of 10	17.27	17.27
M4 × 0.78, 30 mm bolts	pkg of 5	3.71	3.71
M5 × 0.8, 14 mm bolts	pkg of 100	14.92	14.92
M4 × 0.7 hex nut	pkg of 100	3.11	3.11
DIN rail	2	4.57	9.14
Total			**$178.18**

Table 4
Electrical bill of materials summary.

Component	Qty	Cost per unit (USD)	Total cost (USD)
Digital stepper driver	1	22.35	22.45
100W 24V power supply	1	11.03	11.03
Nema 23 stepper motor & Gearbox	1	58.43	58.43
Arduino Mega 2560	1	38.00	38.00
12V to 5V buck converter	1	15.99	15.99
18 AWG 3-Prong power cable	1	14.99	14.99
FUTEK©Load cell	1	798.00	798.00
FUTEK©Signal conditioner	2	1500.00	3000.00
FUTEK©Torque sensor	1	3255.00	3255.00
3.5 mm LED's	5	0.30	1.50
Tactile button switch	2	0.38	0.76
10k resistors	5	0.10	0.50
Total			**$7216.65**

5.1. 3D printed parts

The 3D printed components for this build were made with Makerbot TOUGH polylactic acid (PLA) model material and 80% infill density with a rectilinear pattern. Polyvinyl alcohol (PVA) dissolvable support material was used to provide a smooth surface for the force sensor to sit. Almost any material can be used for this but the high infill density is necessary to lessen deformation when load is applied.

5.2. Machined components

The NEMA 23 adapter plate and clamping plate were cut out of 1/8" 316L stainless steel using a waterjet, but could also be cut to size using a bandsaw. The holes and chamfers were made on a manual machining mill.

5.3. Press construction

A 3.5 mm flathead screw driver, as well as 1.5 mm, 2 mm, 5 mm, and 6 mm hex keys are needed for press construction and electronics cabinet assembly. Four (4) M5 flathead screws connect the faceplate to the stepper motor. Fig. 1 provides an exploded isometric view of the assembled design hardware components. The final assembled drill press is shown in Fig. 3(b). The screw heads should sit flush with the face-plate. Install the 10 mm to 8 mm shaft adapter onto the stepper motor using the clamping screw and set screw ensuring the set screw is aligned with the keyway on the shaft. Install the motor on the press stand using the standoff, clamping bracket, and four (4) 8.5 mm M4 socket head cap screws. Do not fully tighten the 8.5 mm fasteners until the load cell assembly is complete. The clamping plate will be fully secured once the shaft has been installed and aligned with the motor. The standoff should be oriented with the slot to the side to allow access to the motor shaft coupler for driveshaft installation and removal.

Care should be taken when installing the through-hole load cell to prevent damage to the signal wire. Loosely secure the cables for the load cell, torque sensor, and stepper motor to the column shaft using cable ties. Once all components are assembled, tighten the cable tie after ensuring enough cable is provided to allow the full travel range of the press. The load cell is inserted in the load cell housing as shown in Fig. 3(a). Use four (4) 35 mm M4 socket head cap screws and nuts to clamp housing cover to the housing. Torque the fasteners in an alternating fashion to apply an evenly distributed load across the load cell. Install the bronze bushings into the housing.

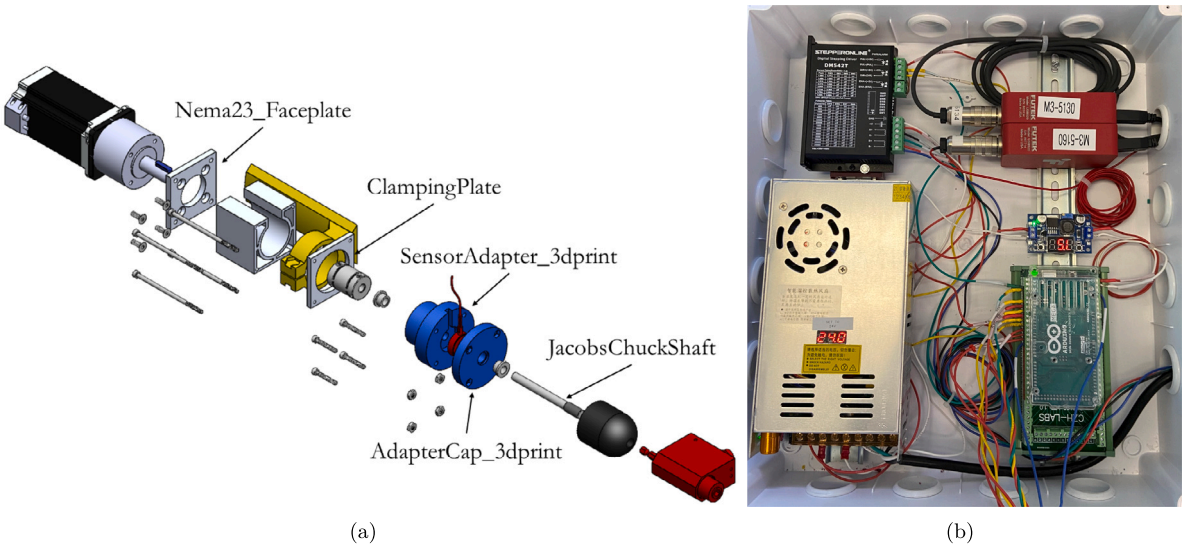

Fig. 1. (a) an isometric view of the assembled build components (b) and the electronics cabinet layout for DIN rail mounts.

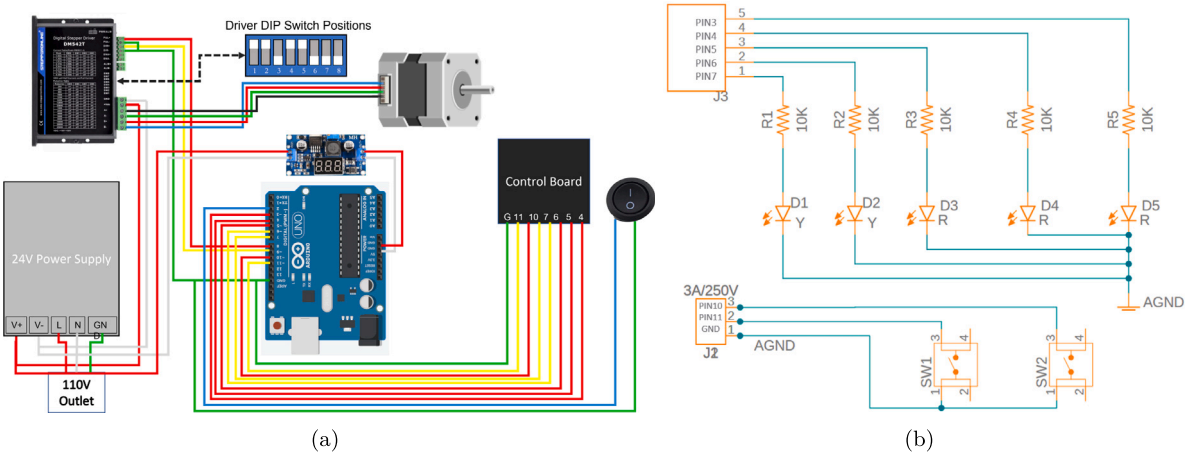

Fig. 2. The (a) overall control schematic and (b) control board wiring schematic.

Use the 6 mm hex wrench to tighten the clamping bolt on the press to hold the load cell housing once it is fully seated. Insert the drill press shaft through the load cell housing and into the adapter. The motor shaft may need to be rotated to allow access to the clamping screws. Once the load cell and shaft have been installed, the four (4) motor fasteners can be fully tightened in a cross pattern. The torque sensor can be installed on the shaft using the two (2) M4 set screws. Ensure that the hex shaft is fully seated in the shaft before tightening set screws.

Optional, the drill press handle can be replaced with a 12-inch pulley to allow for more consistent down force application using counterweights. The drill press handle is removed and the wheel is installed using quick-set epoxy. With the epoxy applied to the handle mount, use a torpedo level to ensure that the wheel is positioned square to the frame. Once the wheel has been properly positioned, a c-clamp may be used to hold the wheel in place until the epoxy cures.

5.4. Electronics assembly

Caution: DO NOT work on any electronics when they are powered on and use caution near the power supply whenever it is plugged in.

All control electronics are mounted on DIN rail inside of a 400 mm by 350 mm electronics enclosure. The DIN rail was mounted directly inside of the box but can also be mounted to a backing plate to allow for easier installation and wiring. Five (5) 3D-printed

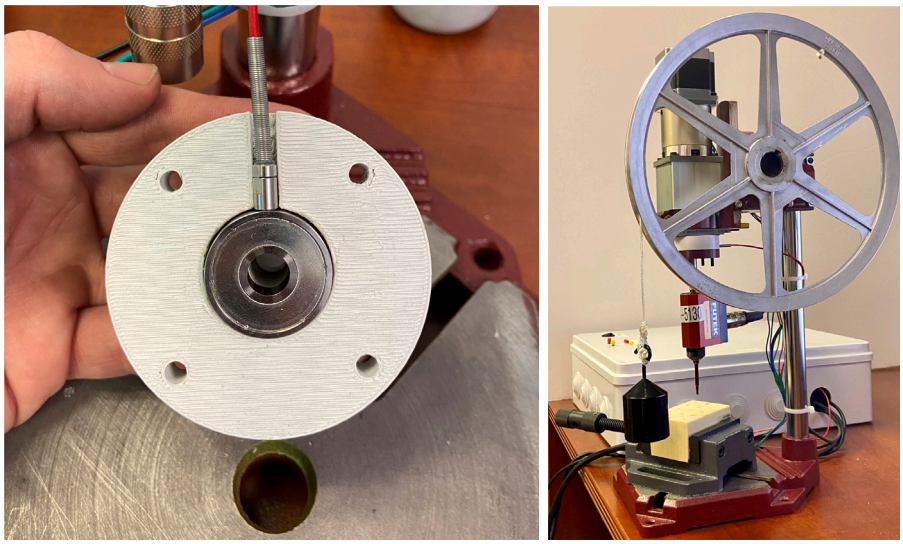

(a) (b)

Fig. 3. The (a) force sensor installation orientation and (b) counterweight setup on downforce pulley.

DIN rail brackets are needed to attach the stepper motor driver and power supply inside of the cabinet. The stepper motor driver was installed with sheet metal screws to the 3D-printed mounts but any screw approximately 12 mm or shorter may be used. The mounts for the power supply were centered on the backside and glued into place using cyanoacrylate (CA) glue. A single DIN rail mount was attached to the buck converter using hot-glue. After mounting all of the components in the cabinet as shown in Fig. 1(b), the DIP switches of the stepper driver should be set to the positions shown in Fig. 2(a). It is good practice to power on the power supply and buck converter to adjust the output voltages before connecting the stepper motor driver or Arduino to prevent over-voltage damage. The components are connected as shown in Fig. 2(b). Holes were drilled in the cabinet lid to place the control board LEDs and buttons through. Alternatively, a small box could be made to hold the board and motor switch that has enough wire to be held or mounted near the press. The on/off switch is held in place with retention clips, while the control board is held in place using hot glue. Ensure that each sensor is connected to its respective signal conditioner.

5.5. Control board construction

The speed and direction control board shown in Fig. 2(a) should be constructed following the wiring schematic shown in Fig. 2(b). This control board can be constructed using a perforated circuit board and soldering components, or could be constructed using a breadboard. Both configurations are detailed further in the project repository. Ensure that current limited resistors are used for all LEDs. Any momentary style switch will work for SW1 and SW2 in Fig. 2(b). A 5 pin and 3 pin JST connector are used for the status light connections and switch connections, respectively.

5.6. Software and firmware installation

The provided Arduino file can be compiled and uploaded to the Arduino MEGA using the Arduino IDE. The Arduino is powered from the buck converter and does not need to be connected to a PC during operation. The SENSIT© software provided with purchase of FUTEK© sensors should be installed onto a Windows PC, following the provided instructions to read data from the sensors. For different speed settings, adjust the variable "microBetweenSteps" in "StepperControl.ino" to adjust the delay between signal pulses in microseconds for the middle speed setting. The low and high speeds are half and twice as fast, respectively, as the medium speed. These are adjustable by changing the constants in the switch block.

6. Operation instructions

Caution: Do not operate the drill press wearing loose clothing, or anything that may get caught in the spindle. Keep long hair tied back, and wear proper PPE. Never adjust the drill press while it is running.

1. Connect the sensor signal conditioners to the data recording PC.
2. Run the SENSIT© software and verify that the sensors are connected and reading properly.
3. Plug in the power cable and switch on the inline switch. Ensure that the power supply is outputting 24 volts and the buck converter is outputting 5 volts.

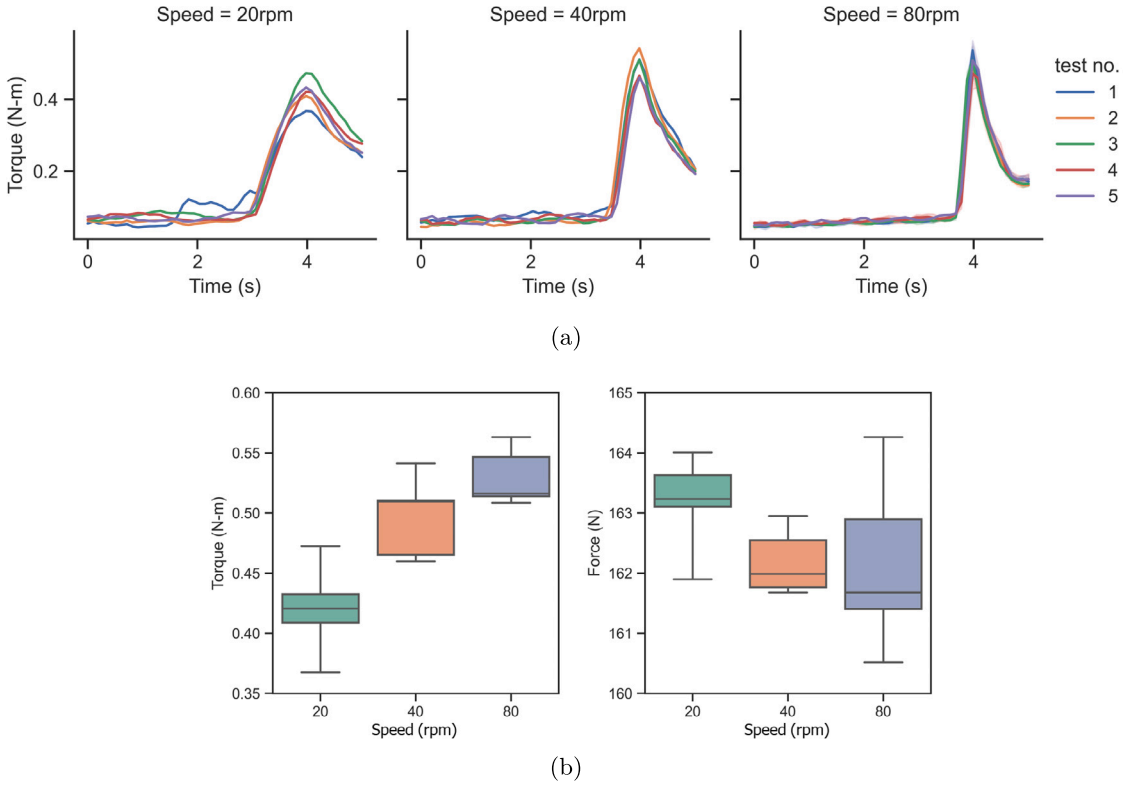

Fig. 4. The (a) torque-time data for five tests (n=5) for 20, 40, & 80 rpm and (b) box plots for the max torque and average down-force for full test duration for each rotational speed during insertion of a 20 mm cortical screw into 20 PCF SAWBONES®.

4. Select the desired rotation speed using the left-side (speed) switch.
5. Select the rotation direction (clockwise/counterclockwise) with the right-side (directional) switch.
6. Install the necessary drive bit into the torque sensor.
7. Configure units (e.g., N, N-m, rpm), test parameters (e.g., sampling rate, test duration, and output filetype and name) in SENSIT©.
8. Before starting test, balance (zero) sensor readings in SENSIT©.
9. Secure insertion material directly beneath torque sensor. Adjust height to accommodate the driver and fastener with an additional 20 mm of clearance to aid in installing the bit and fastener.
10. Once the fastener is placed on the insertion drive bit, start the motor using the on/off switch.
11. Apply downward force by manually rotating handle or using a counterweight system as shown in Fig. 3(b).
12. Switch off motor with the black i/o switch or reverse direction using the direction switch once the screw is fully seated.
13. After screw insertion, stop data recording in SENSIT© software under the "live graph settings" tab.

7. Validation and characterization

This system was validated with test data from bone insertion into SAWBONES® 20 PCF (pound per cubic foot) solid polyurethane foam. Insertion torque and axial force were recorded for five (n=5) runs at three (3) speeds (20, 40, 80 rpm). A 2.5 mm (dia) by 20 mm (length) bone screw was inserted into a 2 mm pilot hole with a steel washer used to simulate a bone plate and prevent the screw head embedding in the material. The screws were inserted until fully stripped to provide a consistent stopping point. Down force was applied using a 300 gram weight suspended from the 12-inch (305 mm) pulley. Fig. 4(a) shows the torque measurements for each run at each speed. Box plots for the peak torque measurements and average axial force are shown in Fig. 4(b). The peak torques for 20, 40, and 80 rpm were 0.420 ± 0.038 N-m, 0.497 ± 0.034 N-m, and 0.530 ± 0.024 N-m, respectively. The combined error for force and torque sensor is 0.87% and 0.30% of rated output, respectively. The force sensor used in this setup has a rated output of 1112 N, which equates to an output accuracy of approximately 10 N. The torque sensor has a maximum output of 18 N-m and a resulting expected accuracy of 0.1 N-m. This was a non-standard test for this material and specific implant, looking at the maximum torque to stripping (failure). Due to this, ASTM F543-17 (Standard Specification and Test Methods for Metallic Medical Bone Screws) was not followed to measure insertion torque [22]. However, this apparatus could be used in compliance with ASTM F543-17, as long as the selected sensors meet the resolution requirement of 10% of the maximum measured torque. For these

validation experiments, the resolution was 25% of the maximum torque with the on-hand sensor. Future experimental tests with higher density bone and bone-analogs will have significantly higher maximum measured torques, most likely resulting in a resolution below 10%. However, if polyurethane foam was the primary material of interest, the FUTEK© TH-605-FSH02038 with a maximum torque rating of 2 N-m would meet the resolution requirement of the standard. In this configuration, the resolution of the apparatus is comparable to the closest commercial analog, the Electroforce© 3200 (with torsion), which can be configured to meet ASTM F543-17 across a wide range of torques and axial loading [23]. It is also has comparable performance to load-frames outfitted with torsion add-ons found in previous literature [8].

- Rotational speeds of 20-80 rpm and up to 120 rpm if motor acceleration is implemented.
- Torque sensor accuracy of 0.1 N-m and force sensor accuracy of 9.6 N. Depending on application and maximum torque/force, other models of the sensors could be selected for high resolution measurements.
- Column working height range 0 mm to 140 mm with torque sensor installed and 0 mm to 216 mm without torque sensor

CRediT authorship contribution statement

J. Logan Betts: Methodology, Investigation, Validation, Writing – original draft, Writing – review & editing. **Frank M. Brinkley:** Methodology, Software, Validation, Formal analysis, Writing – original draft. **Lauren B. Priddy:** Conceptualization, Resources, Writing – review & editing. **Matthew W. Priddy:** Conceptualization, Supervision, Funding acquisition, Writing – review & editing.

Declaration of competing interest

The authors declare that they have no known competing financial interests or personal relationships that could have appeared to influence the work reported in this paper.

Acknowledgments

We thank Nishiana Heard, Elizabeth Holliday, Jonathon Hubbert, Jameelah Jones, and Jalen Mosley for their research and initial experiments. We thank Loubna Ifqir for pilot testing and her thoughtful feedback on previous iterations. We also want to acknowledge FUTEK Advanced Sensor Technology, Inc. for their support of this project. This work was financially supported by the Department of Mechanical Engineering at Mississippi State University.

References

[1] S. Larsson, Treatment of osteoporotic fractures, Scand. J. Surg. 91 (2002) 140–146.
[2] P.V. Giannoudis, V.P. Giannoudis, Far cortical locking and active plating concepts: new revolutions of fracture fixation in the waiting?, Injury 48 (12) (2017) 2615–2618.
[3] A. Gefen, Optimizing the biomechanical compatibility of orthopedic screws for bone fracture fixation, Med. Eng. (2002) 11.
[4] F. Rozema, E. Otten, R. Bos, G. Boering, J. van Willigen, Computer-aided optimization of choice and positioning of bone plates and screws used for internal fixation of mandibular fractures, Int. J. Oral Maxillofac. Surg. 21 (1992) 373–377.
[5] C.-L. Chang, C.-S. Chen, C.-H. Huang, M.-L. Hsu, Finite element analysis of the dental implant using a topology optimization method, Med. Eng. Phys. 34 (2012) 999–1008.
[6] Y.N. Becker, N. Motsch, J. Hausmann, U.P. Breuer, Hybrid composite pedicle screw - finite element modelling with parametric optimization, Inform. Med. Unlocked 18 (2020) 100290.
[7] M. Satpathy, Y. Duan, L. Betts, M. Priddy, J. Griggs, Effect of bone remodeling on dental implant fatigue limit predicted using 3d finite element analysis, J. Dent. Oral Epidemiol. (2022).
[8] F. Addevico, M. Morandi, M. Scaglione, G.F. Solitro, Screw insertion torque as parameter to judge the fixation. assessment of torque and pull-out strength in different bone densities and screw-pitches, Clinical Biomechanics 72 (2020) 130–135.
[9] W.M. Ricci, P. Tornetta, T. Petteys, D. Gerlach, J. Cartner, Z. Walker, T.A. Russell, A comparison of screw insertion torque and pullout strength, Journal of Orthopaedic Trauma 24 (6) (2010) 374–378.
[10] C. Udomsawat, P. Rungsiyakull, C. Rungsiyakull, P. Khongkhunthian, Comparative study of stress characteristics in surrounding bone during insertion of dental implants of three different thread designs: A three-dimensional dynamic finite element study, Clin. Exp. Dent. Res. 5 (2019) 26–37.
[11] Z. Horak, P. Tichy, K. Dvorak, M. Vilimek, Application of an arbitrary lagrangian eulerian method to modelling the machining of rigid polyurethane foam, materials 14 (2021) 1654.
[12] G.R. Johnson, W. Cook, A constitutive model and data for metals subjected to large strains, high strain rates, and high temperatures, in: Proceedings 7th International Symposium on Ballistics, 1983, pp. 541–547.
[13] T.C. Ryken, J.D. Clausen, V.C. Traynelis, V.K. Goel, Biomechanical analysis of bone mineral density, insertion technique, screw torque, and holding strength of anterior cervical plate screws, vol. 83, no. 2, 1995, pp. 324–329.
[14] R. Zdero, T. MacAvelia, F. Janabi-Sharifi, Force and torque measurements of surgical drilling into whole bone, in: Experimental Methods in Orthopaedic Biomechanics, Elsevier, 2017, pp. 85–100.
[15] T.M. Cleek, K.J. Reynolds, T.C. Hearn, Effect of screw torque level on cortical bone pullout strength, Journal of Orthopaedic Trauma 21 (2) (2007) 117–123.
[16] K. Lawson, J. Brems, Effect of insertion torque on bone screw pullout strength, Orthopedics 24 (2001) 451–454.
[17] J. Wilkie, P.D. Docherty, T. Stieglitz, K. Moller, Investigating Torque-Speed Relationship of Self-Tapping Screws, IEEE, 2021, pp. 4383–4386.
[18] F. Affes, H. Ketata, M. Kharrat, M. Dammak, How a pilot hole size affects osteosynthesis at the screw–bone interface under immediate loading, Medical Engnieering and Physics 60 (2018) 14–22.
[19] K. Gok, A. Gok, Y. Kisioglu, Optimization of processing parameters of a developed new driller system for orthopedic surgery applications using taguchi method, International Journal of Advanced Manufacturing Technology 76 (2015) 1437–1448.
[20] J. Lee, B.A. Gozen, O.B. Ozdoganlar, Modeling and experimentation of bone drilling forces, Journal of Biomechanics 45 (6) (2012) 1076–1083.

[21] W.A. Lughmani, K. Bouazza-Marouf, I. Ashcroft, Drilling in cortical bone: a finite element model and experimental investigations, Journal of the Mechanical Behavior of Biomedical Materials 42 (2015) 32–42.
[22] ASTM F543-02, Specification and Test Methods for Metallic Medical Bone Screws, Annual Books of ASTM Standards, ASTM International, 2017.
[23] T. Insturments, Electroforce® load frame and testbench instruments, 2022.

Matthew W. Priddy is an associate professor in the Department of Mechanical Engineering at Mississippi State University (MSU). He received his B.S. and M.S. in Civil Engineering from MSU before obtaining a Ph.D. in Mechanical Engineering from the Georgia Institute of Technology in 2016. Dr. Priddy is the PI of the Computational Mechanics and Materials Laboratory (CMML) at MSU. The primary research focus of CMML is the finite element modeling of complex phenomena (e.g., additive manufacturing, large deformation processes) and advanced material modeling of various material classes (e.g., metals, polymers) for the purpose of translating knowledge from research-based simulations to a tractable format for the larger engineering community. Additionally, CMML has multiple biomedical-related collaborations that include modeling and experimentation of bone fasteners, implant degradation, and bone remodeling.